

Feature Behavior of Resistivity in Bi Foils Obtained by a Melt Spinning Method

Gennadiy N. Kozhemyakin*^{ORCID}, Stanislav Y. Kovalev^{ORCID}

Bi foils with 9-40 μm thicknesses were obtained by a melt spinning method. The microstructure and resistivity in Bi foils at cryothermal treatment have been studied. The foil samples were characterized using XRD to identify the plane orientations and SEM to observe the morphology. The resistivity of Bi foils was measured by two-point probe method at temperatures of 77-300 K using a laboratory cryostat. The formation of Bi polycrystalline foils with a specific orientation allowed us to discover SMSC (Semimetal-Semiconductor Transition) in Bi foils with a 9 μm and 11 μm thicknesses at temperatures of 180-220 K. It was observed that cryogenic cycling increases the resistivity in Bi foils by a factor of 6-19. The experimental results showed that cryothermal treatment provided exfoliation of Bi bilayers with appearance charge carriers and surface conductivity in Bi foils that can be used for real applications in microelectronic components.

Introduction

Topological insulators are a new scientific approach that has practical interest for applications such as enhanced electronic components in integrated circuit technology, high-efficiency thermoelectric convertors, spintronics, superconductivity, more efficient computer memory and improved quantum computer designs [1-5]. In their topological state, these materials exhibit quantum effects that can be observed primarily in layered metals [6]. The formation of conducting one-dimension channels, which develop at the edges of these materials, can provide charge carriers that can be transported without energy dissipation [7]. Most topological materials are composed of heavy metals. Here, heavy semimetal bismuth is one promising topological material. Bismuth in single crystals, ultrafine films and nanostructures is intriguing for its electrical transport properties because of the variety of quantum effects that can be observed [8-21]. It is known that the achievement of the unique physical properties of Bi depends on the element's crystalline structure perfection. The rhombohedral crystal structure of Bi is very sensitive to external influences, including heat field changes [20-24]. Bi and $\text{Bi}_{1-x}\text{Sb}_x$ alloys of single crystals, which are used for the investigation of physical and thermoelectric properties,

have been grown by zone melting, the Bridgman and Czochralski methods [25-29]. A quartz ampoule used in zone melting and the Bridgman method, however, limits Bi expansion in crystal growth, creating large internal tensions in the single crystal that decreases its electro-physical properties. In the Czochralski method, the crystals do not contact the crucible wall, hence providing lower internal tensions and high thermoelectric and physical properties. Therefore, high thermoelectric properties and magnetoresistance can be achieved in Bi and $\text{Bi}_{1-x}\text{Sb}_x$ single crystals grown using the Czochralski technique [30]. Large magnetoresistance can be achieved in Bi films, but this also depends on the perfection of their crystalline structure [15]. A SMSC transition and quantum-size effects can be predicted and observed in Bi films with a thickness of less than 0.03 μm at low and room temperatures [13,31-35]; these films were prepared using the thermal evaporation of a Bi single crystal on mica substrates and by using molecular beam epitaxy on (111) B CdTe substrates. However, these substrates have lattice parameters that are different from Bi that could influence the film crystalline structures and their properties. A melt spinning method is a possible technique for the preparation of thin films. This method is a high-throughput and inexpensive method for the fabrication of metallic glasses as amorphous bulk samples, thin ribbons and films with different properties [36]. Usually, these metallic glasses are microscopically homogeneous and isotropic. Previously, Bi has not been researched because the single-component systems are very difficult to obtain when using this method [37]. Therefore, studying such Bi samples may reveal their unique properties regarding their topological aspects. It is well-known from previous experiments that cryothermal cycling influences the mechanical properties of metallic glasses

Shubnikov Institute of Crystallography of Federal Scientific Research Center "Crystallography and Photonics" of Russian Academy of Sciences, Moscow, Russia

*Corresponding author:

E-mail: genakozhemyakin@mail.ru; Tel.: +79107051917

DOI: 10.5185/amlett.2021.071646

[38,39]. Therefore, cryothermal treatment can be useful for studying the topological state of Bi samples. In the present work, a melt spinning method was applied to obtain Bi foils with different thicknesses ranging from 9–40 μm . The influence of the thickness, microstructure and cryothermal treatment of Bi foils on their resistivity at the temperatures from 300 K to 77 K was studied.

Experimental

Materials/ chemicals details

Bi of 99.9999% purity was used as the source material. It is known that Bi may be oxidized in air at elevated temperatures. Therefore, before using the Bi charge, it was purified by drop cleaning in a vacuum, followed by directional crystallization. Drop cleaning and crystallization were performed in quartz glass ampoules, evacuated up to 10^{-6} mbar (Fig. 1). The cleaning apparatus consisted of a container and two quartz glass ampoules. Top ampoule had a capillary with 2 mm inner diameter and 10 mm height at the bottom. Molten bismuth flowed through the capillary in bottom quartz glass ampoule. Bi melt was heated to 500 $^{\circ}\text{C}$ and held at temperature for 1 hour. Then, the heater moved up at 10 mm/h, and Bi directionally solidified. After that, a Bi polycrystals were obtained in pieces smaller than 7 g.

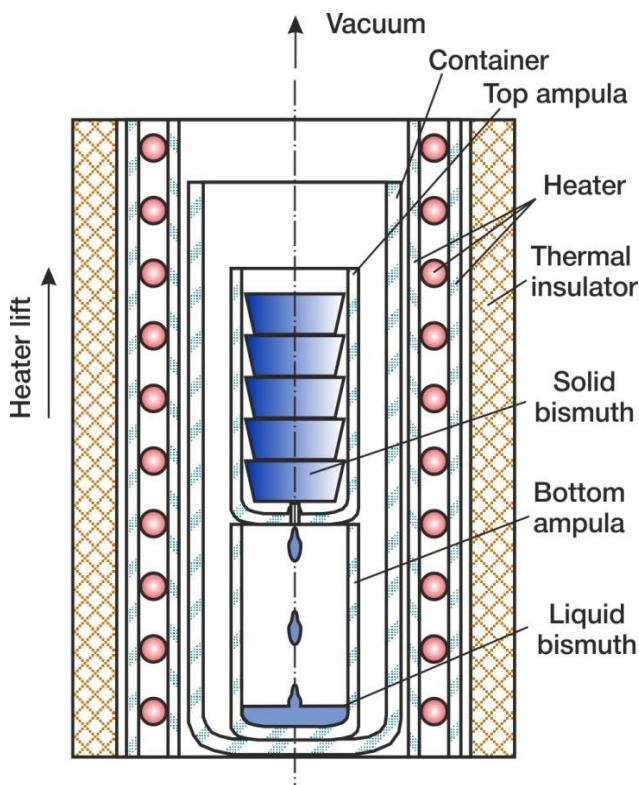


Fig. 1. Schematic drawing of the apparatus for Bi purification.

Material synthesis

The Bi foils were obtained by a melt spinning method. The setup for the preparation of the Bi foils by a melt spinning

method is shown in Fig. 2. Polycrystalline pieces were placed into a quartz ampoule with a 115 mm length, 20 mm inner diameter and constriction to 8 mm at its ends. This ampoule had an external resistance heater and an outer ceramic thermal insulator. High-purity Ar at a gauge pressure of 0.1 atm was passed through the ampoule to prevent Bi melt oxidation. The melt temperature ranging from 300–400 $^{\circ}\text{C}$ was controlled during the spinning process. After Bi had melted and a steady state had been established, the melt was poured out onto a cold copper disc with a 300 mm diameter, rotating at 1100 rpm.

Bi formed as a foil with a thickness up to 40 μm on a copper disc, which further was fell on an aluminium plate.

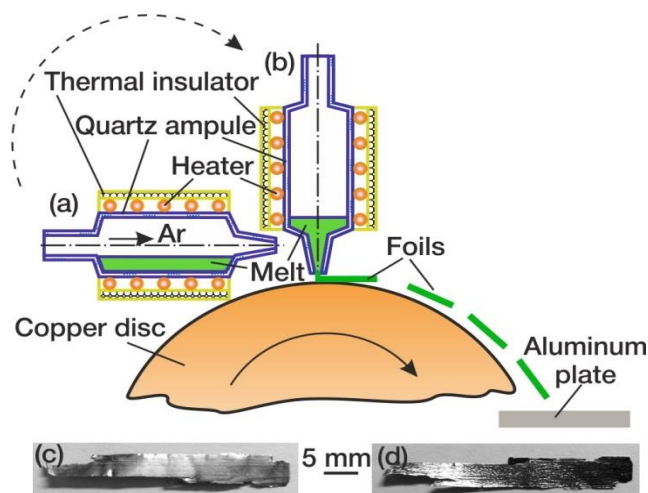


Fig. 2. Schematic drawing of the setup. (a) Melting of Bi polycrystal; (b) Bi melt poured onto a cold copper disk; (c) Foil surface contacting the copper disk; (d) Foil surface did not contact the copper disk.

Characterizations

A cross section of the foils for studying its microstructure was prepared by breaking the samples in liquid nitrogen. The microstructures of as-spinning Bi foils were investigated using an X-ray diffraction method (XRD, XPERT PRO PANalytical) and by a scanning electron microscope (SEM) Quanta 200 3D. The thickness of Bi foils was determined in a cross section using SEM.

The two-point probe method was used for resistivity measurements. The electrical contacts were fixed silver glue cured at room temperature. The resistivity ρ was obtained by applying an electric current I of 1.7 mA through the two end contacts and monitoring the voltage drop between the two probes on a flat surface of the specimens. The resistivity ρ of Bi single crystal and foils was measured at temperatures ranging from 77–300 K using a laboratory cryostat. The temperature dependencies of the Bi foil resistivity were compared with the resistivity of the Bi single crystal, which was grown using the Czochralski technique [29]. The specimen of the Bi single crystal had the form of a rectangular parallelepiped with dimensions of $3 \times 4 \times 15 \text{ mm}^3$ for the measurement of ρ . The current I was applied along the trigonal axis of the specimen. The charge-

carrier density n and mobility μ in the Bi foil with a thickness of 40 μm were measured using the Hall measurement in 0.33 T magnetic field with 7 mA electrical current through the two end contacts of the foil [40]. These measurements confirmed that Bi foils have an n -type conductivity.

Results and discussion

Bi has a rhombohedral primitive unit cell containing two atoms as shown in Fig. 3(a) [20]. Bi crystalline is layered material in the (111) direction and consists of bilayers shown in Fig. 3(b) and Fig. 3(c). The interbilayer bonding in this direction is a weak van der Waals-like bonding [22]. Therefore, Bi single crystals are brittle and easily cleave along the (111) plane [21].

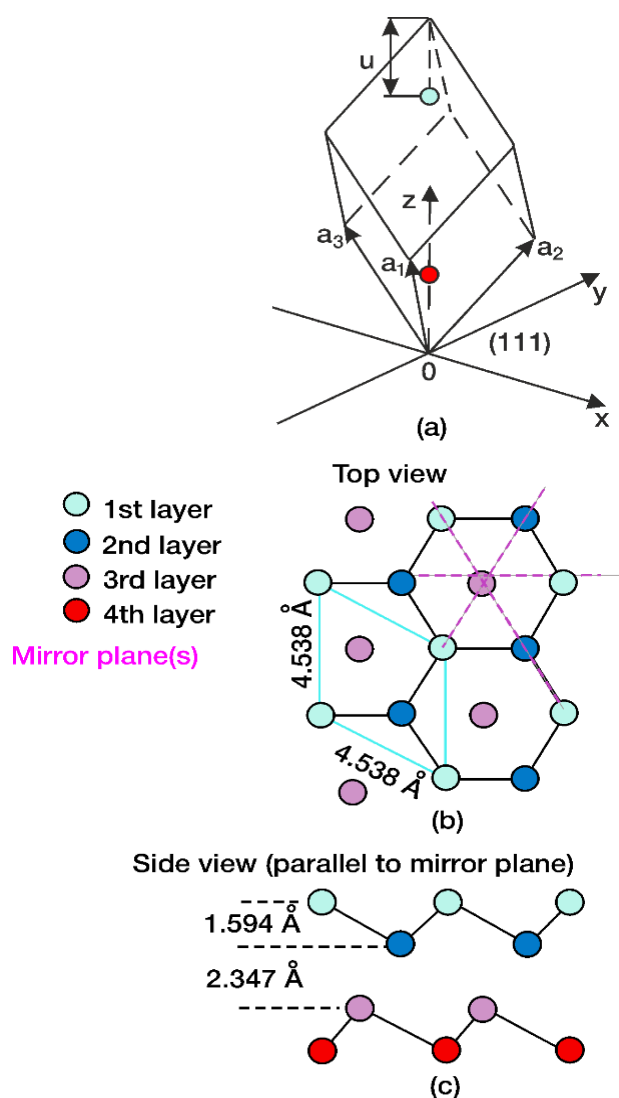


Fig. 3. Characterization of Bi crystalline structure. (a) The rhombohedral unit cell of the Bi crystal containing two atoms. The axes x , y and z are the diad, bisectrix and trigonal axes, respectively [20]. (b) Top view of the first three atomic layers. Each layer consists of a 2D trigonal lattice, and the lattice constants are given. The mirror planes of the structure are also shown as dashed lines. (c) Side view (projected onto a mirror plane) of the first four layers [22].

After spinning process, Bi foils were in as-flake form with 15–40 mm length and 3–5 mm width. The foil surface, which was in contact with the copper disc in the cooling moment, had a smooth shape is shown in Fig. 2(c), and (d), however, show that the foil surface with the contrary hand had wavelike influxes. These Bi foils with 9–40 μm thickness were the polycrystals with crystallites in size from 1–30 μm shown in Fig. 4(a) and Fig. 4(b), and Fig. 4(c). Most crystallites had an oblong shape with flat lateral sides. Twins were observed in the foils with 40 μm thickness is shown in Fig. 4(c). A cross section of Bi foils demonstrates layered microstructure in crystallites with different orientation, as shown in Fig. 4(d) and Fig. 4(e). Layer surfaces in the crystallites are parallel to Bi(111) plane. The splits between these layers are confirmed by the mechanical properties of Bi, which is easily cleaves along the (111) plane [22,23].

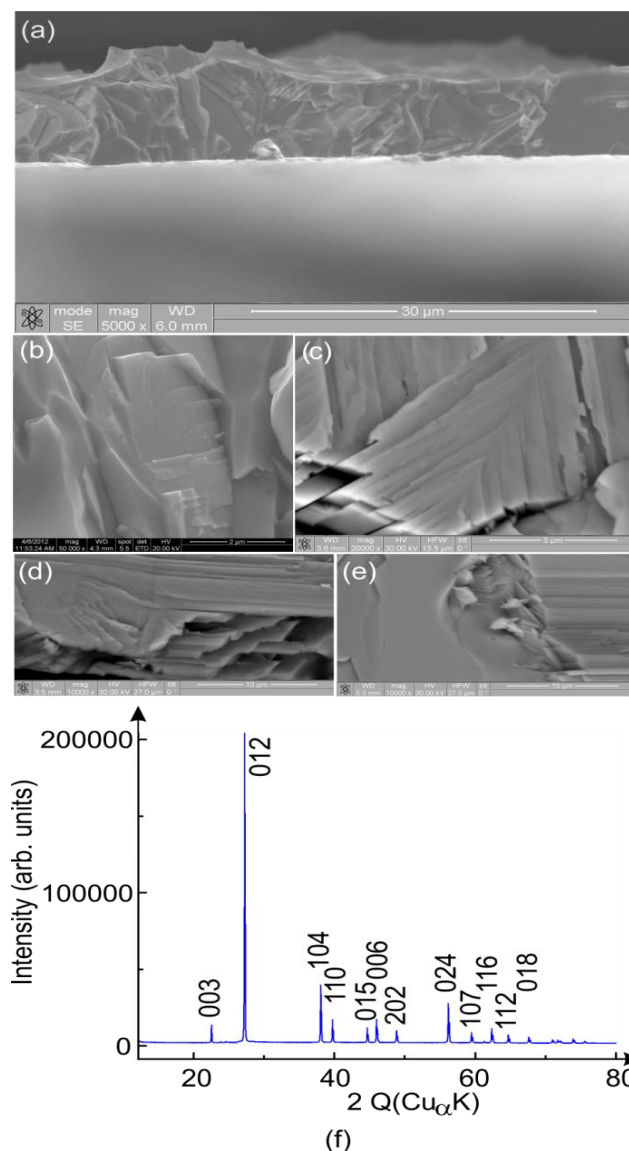


Fig. 4. SEM image of Bi foils with the thickness: (a) 9 μm ; (b) 11 μm ; (c) 40 μm ; (d) 30 μm ; (e) 30 μm ; (f) X-ray diffraction pattern Bi foil with a 11 μm thickness.

Additionally, after a spinning process, most crystallites were orientated in the (111) plane perpendicularly to the Bi foil surface. Bi(111) planes in the crystallites were observed as atomically smooth flat surfaces after being broken in liquid nitrogen as shown in Fig. 4(a), Fig. 4(b) and Fig. 4(e). This is confirmed by the fact that Bi(111) is the natural cleavage plane of Bi crystals [21]. The crystallites with this orientation were formatted at the spinning process because of the high cooling rate and large heat conduction anisotropy of the Bi crystalline structure with its maximal heat conduction being parallel to the (111) plane [26]. The high performance of the foil microstructure with a 11 μm thickness was demonstrated by XRD and is shown in Fig. 4(f).

Fig. 5 shows the temperature dependences of ρ along the length of the Bi foils and trigonal axis of the Bi single crystal. The value of ρ decreases linearly in a Bi single crystal and in Bi foils with a thickness larger than 21 μm as the temperature decreases to 77 K. These dependencies had a metal-like character. The large differences of ρ in Bi single crystal and Bi foils can be the result of their microstructural differences. More importantly, Bi foils with 9 μm and 11 μm thicknesses had temperature dependences of ρ with a SMSC transition at temperatures less than 220 K. A similar SMSC transition was found in very thin Bi films with a 0.03–0.04 μm thickness [31–35]. This SMSC transition can be the result of a unique conducting surface state, which was predicted in $\text{Bi}_x\text{Sb}_{1-x}$ alloys and other topological insulators [41–43]. Decreasing the temperature to 77 K decreases the carrier densities from $2.6 \times 10^{21} \text{ cm}^{-3}$ to $1.1 \times 10^{21} \text{ cm}^{-3}$ and $3.7 \times 10^{21} \text{ cm}^{-3}$ to $0.9 \times 10^{21} \text{ cm}^{-3}$, and increases the carrier mobilities from $10 \text{ cm}^2\text{V}^{-1}\text{s}^{-1}$ to $24 \text{ cm}^2\text{V}^{-1}\text{s}^{-1}$ and from $11 \text{ cm}^2\text{V}^{-1}\text{s}^{-1}$ to $37 \text{ cm}^2\text{V}^{-1}\text{s}^{-1}$ in Bi foils with 9 μm and 11 μm thicknesses, respectively.

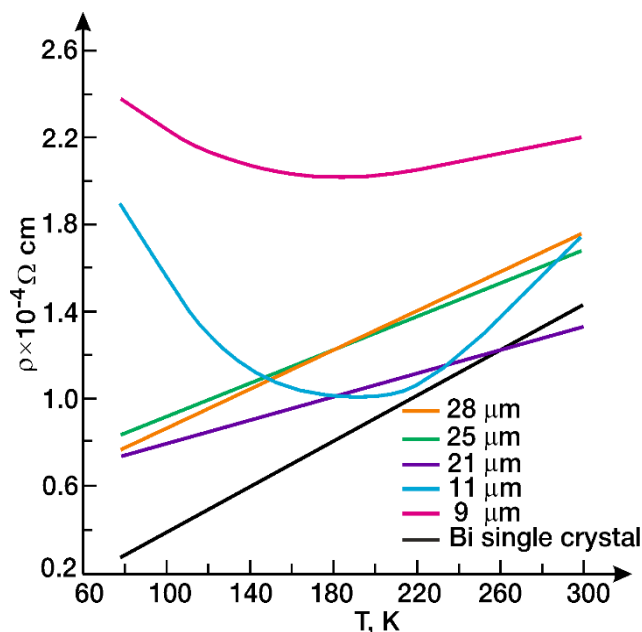


Fig. 5. Temperature dependency of ρ Bi single crystal and Bi foils with thicknesses ranging from 9–28 μm.

We studied the influence of cryothermal treatment on ρ change in Bi foils with 11 μm and 40 μm thicknesses. The ρ in the Bi foils increase from 20% to 200% every time the temperature decrease to 77 K. The ρ increase in the 40 μm foil was observed by a factor of 6–7 at temperatures of 77–300 K after the fifth cryocycle. The largest increase of ρ by a factor of 19 was found in the 11 μm Bi foil at 77 K after the fourth cryocycle (Fig. 6a). The destruction of the foils occurred after 4 (11 μm) and 5 (40 μm) cryogenic cycles.

It is worthwhile to note that cryogenic cycling increase only the voltage drop between the two probes on a sample surface when there was a 1.7 mA constant current. As a result, the voltage drop increase to 5 V for the 3 mm distance between the probes in the 40 μm foil before degradation at 77 K.

However, the increase of the ρ in the 11 μm Bi foil at a temperature of 77 K for four cryogenic cycles is shown in Fig. 6(a) can be the result of a gap increase in the band structure and surface state [32,41,44]. Therefore, we calculated the thermal activation energy gap E_g in 11 μm Bi foil to study the band evolution. We used the line section of the dependencies $\text{Ln}(\rho) \sim T^{-1}$ to calculate E_g according to the equation [45]:

$$\rho(T) = \rho_0 \exp[E_g / (2k_B T)], \quad (1)$$

where, $\rho(T)$ and ρ_0 is resistivity for temperatures of 77–110 K, and k_B is the Boltzmann constant. The E_g for the first and fourth cryocycle in the 11 μm foil were 13 meV and 15 meV, respectively. Thus, this change of E_g values in Bi foils during cryothermal treatment cannot affect the large increase of ρ . However, the ρ experimental measurements show an increase in the voltage drop between the probes on Bi foil surface at cryogenic cycling.

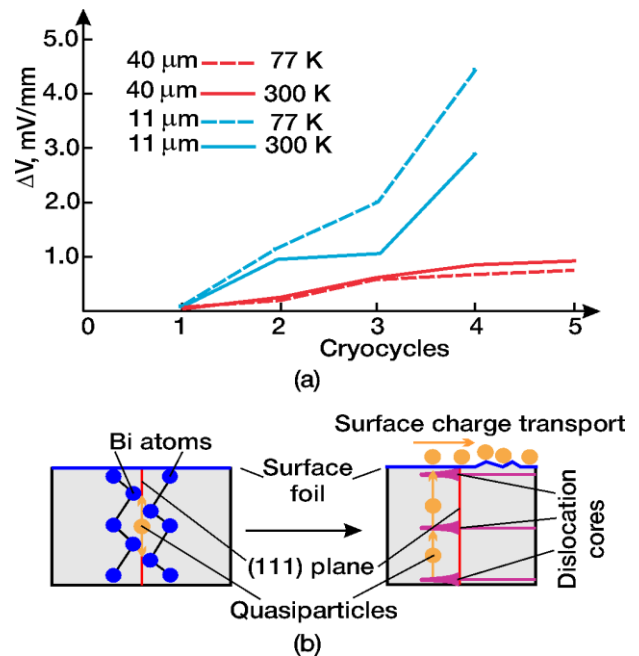


Fig. 6. Dependency of the voltage drop ΔV on cryothermal cycling for Bi foils with thicknesses of 11 μm and 40 μm at temperatures of 77 K and 300 K as shown in Fig. 6(a). Schematic image of the exfoliation in the Bi(111) bilayers with appearance and transport of charge quasiparticles as shown in Fig. 6(b).

As shown in Figure 4(d) and Figure 4(e), the exfoliation Bi foils is the result two causes. First, the interbilayer coupling is about 10 times weaker than the interbilayer covalent bonding. Second, the interbilayer spacing is more affected by temperature [23,24]. A high cooling rate (10^5 - 10^6 K s⁻¹) during the melt spinning process produces thermal strain in Bi foils, which caused the exfoliation of Bi(111) bilayers and appearance of the cracks parallel to (111) plane. The subsequent cryothermal treatment amplify the exfoliation of Bi(111) bilayers.

Based on these experiments, we assume that cryothermal treatment that causes the exfoliation of the Bi(111) bilayers can be provide the appearance of charge quasiparticles, as predicted for Bi and by ultrathin Bi(111) films [35-38]. The exfoliation of Bi(111) bilayers with weak van der Waals type inter-bilayer bond contribute generation charge quasiparticles that tunnel through the 1D modes near dislocation core to a foil surface [46,47]. Apparently that the appearance of these quasiparticles (Fig. 6(b)) causes the increase of the voltage drop and demonstrates the increase of surface conductivity characteristic for topological insulators. Importantly, Bi is a heavy semimetal, having a honeycomb lattice and a layered microstructure, which are the basic characteristics of topological insulators.

Conclusion

In this work, we developed the conditions for obtain of Bi foils by a melt spinning method. Experimentally, it was shown that Bi foils with 9–40 μm thicknesses had layered polycrystalline structures with 1–30 μm dimension crystallites. Most crystallites had an orientation with the (111) plane perpendicular to the foil surface. It was established that the temperature dependences of resistivity for Bi foils with thicknesses larger than 21 μm at temperatures of 77–300 K had a linear characteristic similar to Bi single crystals. A SMSC transition was found in Bi films with 9 μm and 11 μm thicknesses at temperatures near 180 K and 220 K, respectively. Probably, these SMSC transitions in Bi foils occurred because of a gap appearing in the band structure and topological surface state. Cryogenic cycling up to five times at when decreasing the temperature to 77 K increased the resistivity in Bi foils by a factor of 6–19. A significant increase in the voltage drop on the foil surface as detected using a resistivity measurement could be the result of special charge carriers surface states. This state can be caused by cryothermal treatment, which causes exfoliation of the Bi(111) bilayers and the appearance of charge quasiparticles increasing surface conductivity. Bi foils possess the characteristic properties of topological insulators and can be used for the potential future applications in microelectronic components.

Acknowledgements

The authors are thankful to Dr. O.N. Soklakova and Dr. V.V. Artemov for the images of the cross section of Bi foils. The authors thank Dr. S.N.

Sulyanov for the results of X-ray investigations. This work was supported by the Ministry of Science and Higher Education within the State assignment FSRC “Crystallography and Photonics” RAS.

Conflicts of interest

The authors whose names are listed state that they have no conflicts to declare.

Keywords

Bismuth foils, topological insulators, melt spinning method, cryothermal treatment.

Received: 10 September 2020

Revised: 9 February 2021

Accepted: 13 February 2021

References

1. Savage, N.; *ACS Cent. Sci.*, **2018**, *4*, 523.
2. Wang, J.; Zhang, S.C.; *Nat. Mat.*, **2017**, *16*, 1062.
3. Wang, X.L.; Dou, S.X.; Zhang, C.; *NPG Asia Mater.*, **2010**, *2*, 1, 31.
4. Ando, Y.; *J. Phys. Soc. Jpn.*, **2013**, *82*, 102001.
5. Li, C.; Boer, J. C.; Ronde, B.; Ramankutty, S.V.; Heumen, E.; Huang, Y.; Visser, A.; Golubov, A.A.; Golden, M.S.; Brinkman, A.; *Nat. Mat.*, **2018**, *17*, 875.
6. Klitzing, K.; Dorda G.; Pepper M.; *Phys. Rev. Lett.*, **1980**, *45*, 494.
7. König, M.; Wiedmann, S.; Brüne, C.; Roth, A.; Buhmann, H.; Molenkamp, L.W.; Qi, X.L.; Zhang, S.C.; *Science*, **2007**, *318*, 766.
8. Mase, S.; *J. Phys. Soc. Japan*, **1959**, *14*, 5, 584.
9. Baraff, G.A.; *Phys. Rev.*, **1965**, *137*, 3A, A842.
10. Brandt, N.B.; Dolgolenko, T. F.; Stupochenko, N.N.; *Sov. Phys. JETP*, **1964**, *18*, 908.
11. Patthey, F.; Schneider, W.-D.; Micklitz, H.; *Phys. Rev. B*, **1994**, *49*, 16, 11293.
12. Dey, K.K.; Banerjee, D.; Bhattacharya, R.; *J. Magn. Magn. Mater.*, **2004**, *268*, 140.
13. Komnik, Yu.F.; *Physics of Metallic Films*; Atomizdat, Moscow, USSR, **1979**.
14. Butenko, A.V.; Sandomirsky, V.; Schlesinger, Y.; Shvarts, Dm.; Sokol, V.A.; *J. Appl. Phys.*, **1997**, *82*, 1266.
15. Yang, F.Y.; Liu, K.; Chien, C.L.; Searson, P.C.; *Phys. Rev. Lett.*, **1999**, *82*, 3328.
16. Yang, F.Y.; Liu, K.; Hong, K.; Reich, D.H.; Searson, P.C.; Chien, C.L.; *Science*, **1999**, *284*, 1335.
17. Chang, J.; Kim, H.; Han, J.; Jeon, M.H.; Lee, W.Y.; *J. Appl. Phys.*, **2005**, *98*, 023906.
18. Zhang, Z.; Sun, X.; Dresselhaus, M.S.; Ying, J.Y.; Heremans, J.; *Phys. Rev. B*, **2000**, *61*, 4850.
19. Dresselhaus, M.S.; Chen, G.; Tang, M.Y.; Yang, R.; Lee, H.; Wang, D.; Ren, Z.; Fleurial, J.P.; Gogna, P.; *Adv. Mater.*, **2007**, *19*, 1043.
20. Saikawa, K.; *J. Phys. Soc. Jap.*, **1970**, *29*, 562.
21. Ast, C.R.; Höchst, H.; *Phys. Rev. B*, **2003**, *67*, 016403.
22. Mönig, H.; Sun, J.; Koroteev, Yu. M.; Bihlmayer, G.; Wells, J.; Chulkov, E.V.; Pohl, K.; Hofmann, Ph.; *Phys. Rev. B*, **2005**, *72*, 085410.
23. Hofmann, Ph.; *Prog. Surf. Sci.*, **2006**, *81*, 191.
24. Sabater, C.; Gosalbez-Martinez, D.; Fernandez-Rossier, J.; Rodrigo, J.G.; Untiedt, C.; Palacios, J.J.; *Phys. Rev. Lett.*, **2013**, *110*, 176802.
25. Brown, D.M.; Heumaun, F.K.; *J. Appl. Phys.*, **1964**, *35*, 6, 1947.
26. Jain, A.L.; *Phys. Rev.*, **1959**, *114*, 6, 1518.
27. Kapitza, P.; Method growth of Bi crystals, *Proc. Roy. Soc. A*, **1928**, *119*, 358.
28. Yue, Z.J.; Wang, X.L.; Yan, S.S.; *Appl. Phys. Lett.*, **2015**, *107*, 11, 112101.
29. Zemskov, V.S.; Belaya, A.D.; Beluy, U.S.; Kozhemyakin, G.N.; *J. Cryst. Growth*, **2000**, *212*, 161.
30. Kozhemyakin, G.N.; Zayakin, S.A.; *J. Appl. Phys.*, **2017**, *122*, 205102.
31. Lutskii, V.N.; *JETP Lett.*, **1965**, *2*, 245.
32. Ogrin, Yu.F.; Lutskii, V.N.; Elinson, M.I.; *JETP Lett.*, **1966**, *3*, 71.
33. Hoffman, C.A.; Meyer, J.R.; Bartoli, F.J.; Di Venere, A.; Yi, X.J.; Hou, C.L.; Wang, H.C.; Ketterson, J.B.; Wong, G.K.; *Phys. Rev. B*, **1993**, *48*, 11431.

34. Lu, M.; Zieve, R.J.; Hulst, A.; Jaeger, H.M.; Rosenbaum, T.F.; Radelaar, S.; *Phys. Rev. B*, **1996**, *53*, 1609.
35. Rogacheva, E.I.; Grigorov, S.N.; Nashchekina, O.N.; Lyubchenko, S.; Dresselhaus, M.S.; *Appl. Phys. Lett.*, **2003**, *82*, 2628.
36. Kumar, G.; Desai, A.; Schroers, J.; *Adv. Mater.*, **2011**, *23*, 461.
37. Bhat, M.H.; Molinero, V.; Soignard, E.; Solomon, V.C.; Sastry, S.; Yarger, J.L.; Angell, C.A.; *Nature*, **2007**, *448*, 787.
38. Ketov, S.V.; Trifonov, A.S.; Ivanov, Yu. P.; Churyumov, A.Yu.; Lubchenko, A.V.; Batrakov, A.A.; Jiang, J.; Louzguine-Luzgin, D.V.; Eckert, J.; Orava, J.; Greer, A.L.; *NPG Asia Mater.*, **2018**, *10*, 4, 137.
39. Bu, V.; Wang, J.; Li, L.; Kou, H.; Xue, X.; Li, J.; *Metals*, **2016**, *6*, 274.
40. Werner, F.; *J. Appl. Phys.*, **2017**, *122*, 135306.
41. Fu, L.; Kane, C.L.; Mele, E.J.; *Phys. Rev. Lett.*, **2007**, *98*, 106803.
42. Fu, L.; Kane, C.L.; *Phys. Rev. B*, **2007**, *76*, 045302.
43. Hasan, M.Z.; Kane, S.L.; *Rev. Mod. Phys.*, **2010**, *82*, 3045.
44. Hirahara, T.; Nagao, T.; Matsuda, I.; Bihlmayer, G.; Chulkov, E.V.; Koroteev, Yu.M.; Echenique, P.M.; Saito, M.; Hasegawa, S.; *Phys. Rev. Lett.*, **2006**, *97*, 146803.
45. Pavlov, L.P.; Methods of Determination of Key Parameters of Semiconductor Materials; Vishaya Shkola, Moscow, USSR, **1975**.
46. Ran, Y.; Zhang, Y.; Vishvanath, A.; *Nat. Phys.*, **2009**, *5*, 298.
47. Tretiakov, O.A.; Abanov, Ar.; Murakami, S.; Sinova, J.; *Appl. Phys. Lett.*, **2010**, *97*, 073108.

Authors biography



Prof. Gennadiy Nikolaevich Kozhemyakin serves as a Leading Researcher at the Space Materials Science Laboratory of Shubnikov Institute of Crystallography of Federal Scientific Research Center “Crystallography and Photonics” of Russian Academy of Sciences. He is a high-end professor and has professor titles since 1995. Dr. Kozhemyakin developed of 15 technologies for crystal growth, nanomaterials and 3 original technologies of crystal growth for the Research Institute Electronics and Institute of Space and Astronautical Sciences in Japan.



Post student **Stanislav Yurievich Kovalev** serves at the Space Materials Science Laboratory of Shubnikov Institute of Crystallography of Federal Scientific Research Center “Crystallography and Photonics” of Russian Academy of Sciences. He has actively involve in research of amorphous and crystal materials.

Graphical abstract

A melt spinning method was developed for the formation of Bi foils with 9–40 μm thicknesses. Bi foils had polycrystalline structure with specific orientation of the crystallites. Cryothermal treatment at temperatures of 77–300 K allowed discover exfoliation of the Bi(111) bilayers in these foils that increased the resistivity by a factor up of 6–19 due to surface conductivity increase characteristic for topological insulators.

